ANTIOXIDANTS & REDOX SIGNALING
Volume 14, Number 7, 2011

DOI: 10.1089/ars.2010.3287

Amyloid β-Peptide Oligomers Stimulate RyR-Mediated Ca^{2+} Release Inducing Mitochondrial Fragmentation in Hippocampal Neurons and Prevent RyR-Mediated Dendritic Spine Remodeling Produced by BDNF

Andrea C. Paula-Lima,[1] Tatiana Adasme,[1] Carol SanMartín,[1] Adriano Sebollela,[2] Claudio Hetz,[1,3] M. Angélica Carrasco,[1,4] Sergio T. Ferreira,[2] and Cecilia Hidalgo[1,4]

Abstract

Soluble amyloid β-peptide oligomers (AβOs), increasingly recognized as causative agents of Alzheimer's disease (AD), disrupt neuronal Ca^{2+} homeostasis and synaptic function. Here, we report that AβOs at sublethal concentrations generate prolonged Ca^{2+} signals in primary hippocampal neurons; incubation in Ca^{2+}-free solutions, inhibition of ryanodine receptors (RyRs) or *N*-methyl-D-aspartate receptors (NMDARs), or preincubation with *N*-acetyl-L-cysteine abolished these signals. AβOs decreased (6 h) RyR2 and RyR3 mRNA and RyR2 protein, and promoted mitochondrial fragmentation after 24 h. NMDAR inhibition abolished the RyR2 decrease, whereas RyR inhibition prevented significantly the RyR2 protein decrease and mitochondrial fragmentation induced by AβOs. Incubation with AβOs (6 h) eliminated the RyR2 increase induced by brain-derived nerve factor (BDNF) and the dendritic spine remodeling induced within minutes by BDNF or the RyR agonist caffeine. Addition of BDNF to neurons incubated with AβOs for 24 h, which had RyR2 similar to and slightly higher RyR3 protein content than those of controls, induced dendritic spine growth but at slower rates than in controls. These combined effects of sublethal AβOs concentrations (which include redox-sensitive stimulation of RyR-mediated Ca^{2+} release, decreased RyR2 protein expression, mitochondrial fragmentation, and prevention of RyR-mediated spine remodeling) may contribute to impairing the synaptic plasticity in AD. *Antioxid. Redox Signal.* 14, 1209–1223.

Introduction

Alzheimer's disease (AD) is an age-related neurodegenerative disorder characterized by progressive memory loss that leads inevitably to severe dementia. Numerous reports have linked the pathogenesis of AD, the most frequent cause of dementia worldwide, with the accumulation and aggregation of amyloid beta (Aβ)-peptide in the brain (27, 46); for a review, see (29). Although Aβ monomers are not neurotoxic, local peptide accumulation favors self-association and generation of different Aβ aggregates that include insoluble Aβ fibrils and soluble Aβ oligomers, which have been proven toxic to neurons and other brain cell types (25, 42, 57, 73). Insoluble Aβ fibrils, resembling those found in amyloid plaques, are neurotoxic at micromolar concentrations both *in vitro* and *in vivo* (44, 57). Even more relevant to AD pathology is the fact that soluble Aβ oligomers (hereafter referred to as AβOs) accumulate specifically in AD human brain and cerebrospinal fluid and act as potent and diffusible neurotoxins (42). AβOs associate with synapses (41) and cause a swift increase in intracellular Ca^{2+} concentration ($[Ca^{2+}]$) (14, 17), but the contribution of Ca^{2+}-induced Ca^{2+} release (CICR) from intracellular stores to this $[Ca^{2+}]$ increase has not been investigated in depth. AβOs also impair Ca^{2+}-dependent neuronal functions, increasing tau hyperphosphorylation (16), oxidative stress (14), and excitotoxicity (1a). Significantly, AβOs interfere with synaptic plasticity and inhibit long-term potentiation (LTP), a classic paradigm of memory-associated synaptic mechanisms (42, 73). Functional and morphologic deterioration of synapses by AβOs strongly associate with memory loss in AD (15, 41, 43, 63).

A regulated increase in intracellular $[Ca^{2+}]$ plays key roles in hippocampal synaptic plasticity, whereas disruption of neuronal Ca^{2+} homeostasis is likely to result in neuronal

[1]Centro de Estudios Moleculares de la Célula, Instituto de Ciencias Biomédicas, Facultad de Medicina, Universidad de Chile, Santiago, Chile.
[2]Programa de Bioquímica e Biofísica Celular, Instituto de Bioquímica Médica, Universidade Federal do Rio de Janeiro, Brasil.
Programas de [3]Biología Celular y Molecular and [4]Fisiología y Biofísica, Instituto de Ciencias Biomédicas, Facultad de Medicina, Universidad de Chile, Santiago, Chile.

death (28, 50). Alterations of Ca^{2+} homeostasis by AβOs have been implicated in AD pathogenesis (14, 17); for recent reviews, see (7, 8). Similarly, amyloid precursor protein (APP) (25) or presenilin mutations associated with familial AD may compromise the normal Ca^{2+}-regulating functions of plasma membrane APP or of endoplasmic reticulum (ER)-resident presenilins or both (8).

The three known mammalian RyR isoforms (RyR1, RyR2, and RyR3) are present in mammalian brain (24, 77). Several reports indicate that RyR-mediated Ca^{2+} release contributes to the defective Ca^{2+} homeostasis that accompanies AD pathogenesis. The N-terminus of presenilin-2 increases single-channel activity of brain RyR through direct protein–protein interactions (31). Downregulation of RyR expression, especially of the RyR2 isoform, occurs very early in human AD brain postmortem samples (36), whereas upregulation of RyR3 expression and altered Ca^{2+} signaling have been suggested to occur in different AD transgenic mouse models (65, 66). Moreover, extracellular Aβ leads to increased RyR3 expression in primary cortical neurons (66), whereas treatment of cortical neurons with Aβ fibrils promotes ER Ca^{2+} release through RyR and inositol 1,4,5-trisphosphate receptors, inducing ER stress, oxidative stress, and cell death (20, 60).

Many studies have established that sustained hippocampal neuronal plasticity entails generation and growth of dendritic spines (38). These morphologic changes are mediated by brain-derived neurotrophic factor (BDNF) (13, 67), a neurotrophin synthesized and released from neurons in an activity-dependent manner (40). On binding to TrkB receptors, BDNF stimulates several intracellular signaling cascades, including calcium-dependent kinase pathways (3, 71) that contribute to inducing and maintaining hippocampal LTP (58). Soluble AβOs, which are known to disrupt synaptic plasticity, decrease BDNF mRNA levels and compromise BDNF-induced intracellular signaling (23, 68, 69).

In view of the key roles played by both RyR and BDNF in synaptic plasticity (4, 22, 33, 35, 67) and their potential effects on AD pathology, we studied here the possible effects of AβOs on the generation of RyR-mediated Ca^{2+} signals, RyR expression, and BDNF-induced dendritic spine remodeling. Our results suggest that AβOs, through stimulation of RyR-mediated Ca^{2+} release, engage Ca^{2+}-dependent pathways that downregulate RyR expression, thus preventing RyR-dependent spine growth induced by BDNF or caffeine. We propose that sustained stimulation of RyR-mediated Ca^{2+} release by AβOs represents a significant factor in the synaptotoxicity and synaptic plasticity defects induced by AβOs.

Experimental Procedures

Materials

Aβ peptide (A$\beta_{1–42}$) was purchased from Bachem Inc. (Torrance, CA), and BDNF, from Chemicon Millipore (Billerica, MA). Fluo4-AM, calcein-AM, the Live/Dead viability kit for mammalian cells, ProLong, Alexa Fluor 488 anti-rabbit, and Alexa Fluor 635 anti-mouse were from Molecular Probes, Inc. (Eugene, OR). Trizol reagent was from Invitrogen (Carlsbad, CA). Hexafluoro-2-propanol (HFIP) was from Merck (Darmstadt, Germany); B27 supplement and Neurobasal medium were from Gibco (Carlsbad, CA). Rabbit anti-RyR3 and mouse anti-MAP2 were from Chemicon (Temecula, CA), mouse anti-RyR2 and mouse anti-mHSP70 from Pierce Biotechnology (Rockford, IL), monoclonal anti-$\beta-$actin from Sigma (St. Louis, MO), anti-glial fibrillary acidic protein (GFAP) from DAKO (Carpinteria, CA), rabbit anti-Drp-1 from Thermo Scientific (Rockford, IL), mouse anti-cytochrome *c* from BD Biosciences (San Jose, CA), and rabbit anti-COX IV from Cell Signaling (Danvers, MA). DNA-free Kit was obtained from Ambion (Austin, TX). ImProm-IIReverse Transcriptase kit was from Promega (Madison, WI), the DNA-binding dye SYBR green (Platinum SYBR Green qPCR SuperMix UDG) was from Invitrogen, and PDVF membranes from Millipore. BAPTA and 3-[4,5-dimethylthiazol-2-yl]-2,5-diphenyl tetrazolium bromide (MTT) were from Sigma Chemical, and ionomycin, from Calbiochem (La Jolla, CA).

Preparation of AβOs and Aβ fibrils

The A$\beta_{1–42}$ peptide, prepared as a dried hexafluore-2-propanol (HIFP) film, as described previously (14), was stored at -80°C for up to 4 months. Before use, this peptide film was dissolved in sufficient sterile DMSO to make a 5 m*M* stock solution. To prepare AβOs by using standard methods (41), the 5 m*M* peptide solution was subsequently diluted to 100 μM with cold phosphate-buffered saline (PBS), aged overnight at 4°C, centrifuged at 14,000 *g* for 10 min at 4°C to remove insoluble aggregates (protofibrils and fibrils), and the supernatant containing soluble AβOs was transferred to clean tubes and stored at 4°C. The oligomeric state of AβO preparations was confirmed by Western blot and HPLC analysis, as described (14, 72). Only fresh AβO preparations (1 day old) were used in all experiments. For preparation of Aβ fibrils, the 5 m*M* stock solution of Aβ peptide was diluted 50-fold in 10 m*M* HCl in PBS, immediately vortexed for 30 s, and incubated for 24 h at 37°C as described (14). To check the uniformity of AβO and Aβ fibril preparations, 5 μl of a solution containing 10 μM AβOs or 10 μM Aβ fibrils was applied to Formvar-coated grids, and after 1 min, were washed twice with filtered water. Samples were negatively stained with filtered 2% uranyl acetate for 1 min and imaged by transmission electron microscopy in a Zeiss EM-109 microscope at 80 kV. Supplementary Figure S1A illustrates a representative electron micrograph of an AβO preparation, showing abundant oligomers with the classic spherical morphology previously described (17, 42) and with an average diameter of $\sim$6 nm (Supplementary Data are available online at www.liebertonline.com/ars). Aβ fibrils, which were not observed in fresh AβO preparations, were also successfully generated (Supplementary Fig. S1B).

Primary hippocampal cultures

Cultures were prepared from 18-day-old embryos obtained from pregnant Sprague–Dawley rats, as previously described (52). In brief, brains were removed and placed in a dish containing Hanks-glucose solution. Hippocampi were dissected and, after stripping away meninges membranes, cells were gently dissociated in Hanks-glucose solution, centrifuged, and resuspended in DMEM medium supplemented with 10% horse serum. Dissociated hippocampal neurons were plated on polylysine-coated plates, and after 1 h, DMEM was replaced by Neurobasal medium supplemented with B-27. Cells were incubated for 15 to 21 days *in vitro* (DIV) at 37°C in a humidified 5% CO_2 atmosphere before experimental manip-

ulations. These mature cultures were substantially enriched in neuronal cells, as revealed by immunocytochemistry (Supplementary Fig. S1C), and expressed both RyR2 and RyR3 in neurites and cell bodies (Supplementary Fig. S1D and E).

Immunocytochemistry

Hippocampal cultures (21 DIV) were fixed by adding an equal volume of 4% formaldehyde (in PBS buffer) for 5 min. After this solution was replaced with 4% formaldehyde, cultures were incubated for 10 min, rinsed 3 times with PBS, incubated with 10% normal goat serum plus 0.1% Triton X-100 (blocking-permeant solution) for 1 h, and then immunolabeled by overnight incubation at 4°C with different antibodies diluted in blocking solution. Rabbit anti-RyR3 (1:30,000), mouse anti-RyR2 (1:30,000), mouse anti-MAP2 (1:500), GFAP (1:500), AβOs-selective NU4 mouse monoclonal antibody (44 μg/ml) or anti-cytochrome *c* (1:1,000) was used. After this incubation period, fixed cultures were rinsed 3 times with PBS and incubated for 1 h at room temperature with Alexa Fluor 488 anti-rabbit, Alexa Fluor 635 anti-mouse, or Alexa Fluor 488 anti-sheep as secondary antibodies (1:400 in blocking solution). Cells were rinsed 3 times with PBS, and coverslips were mounted in ProLong or DAKO mounting medium. Cells were visualized on a Carl Zeiss LSM Pascal 5 confocal microscope system (Zeiss, Oberkochen, Germany), and images were digitally acquired by using LSM software (Zeiss). The ImageJ software program (National Institutes of Health, Baltimore, MD) was used for image deconvolution and generation of zeta projections from seven to15 stacks (0.4-μm thickness each). Quantitative analysis of immunofluorescence data was carried out with histogram analysis of the fluorescence intensity at each pixel across the image (after deconvolution) of a selected stack by using the ImageJ software.

Cell-viability assays

The viability of neuronal cultures was determined by using either the Live/Dead assay, as previously described (53), or the MTT reduction assay. For the former assay, culture medium was removed, and cells were gently washed 3 times with PBS-glucose. Cells were then incubated at room temperature for 40 min with PBS-glucose containing 2 μ*M* calcein-AM ester and 1 μ*M* ethidium homodimer and were imaged with a Nikon Eclipse TE300 microscope. Live neurons were identified by their green calcein fluorescence and dead neurons by the red fluorescence of DNA-bound ethidium. Assays were carried out in triplicates with three independent neuronal cultures. Ten randomly chosen fields were examined per culture well, and about 500 cells were counted in each field per experimental condition. The percentage of live neurons was calculated relative to the total number of neurons observed in each field. Neuronal viability (mean ± SEM) is expressed as percentage of live cells relative to control cultures. When using the MTT assay, neuronal cultures were analyzed, as previously described. In brief, to allow MTT reduction to formazan blue by metabolically active cells, cultures were incubated for 4 h at 37°C with MTT (0.5 mg/ml). Cells were then lysed, and formazan crystals were solubilized by overnight incubation at room temperature in 0.01N HCl containing 10% SDS. Optical density at 590 nm was measured in a ThermoMax Microplate reader.

Incubation of primary hippocampal cultures with AβOs

Unless otherwise indicated, neurons maintained in culture for 21 DIV were incubated with AβOs (500 n*M*) for 6 h. In these conditions, significant binding of AβOs to the soma and dendrites was observed (Supplementary Fig. S2A), with a similar punctate distribution, as previously reported (14). Neurons incubated only with saline did not present bound AβOs (Supplementary Fig. S2B).

Determination of intracellular Ca^{2+} signals

Cells were transferred to modified Tyrode solution (in m*M*: 129 NaCl, 5 KCl, 2 $CaCl_2$, 1 $MgCl_2$, 30 glucose, 25 HEPES-Tris, pH 7.3), preloaded for 30 min at 37°C with 5 μ*M* Fluo4-AM and washed 3 times with modified Tyrode solution to allow complete dye deesterification. Fluorescence images of intracellular Ca^{2+} signals in primary hippocampal neurons were obtained every 15 s in an inverted confocal microscope (Carl Zeiss, Axiovert 200, LSM 5 Pascal, Jena, Germany, Plan Apochromatic 63×Oil DIC objective; excitation, 488 nm; argon laser beam). Image data were acquired in cell bodies. Frame scans were averaged by using the equipment data-acquisition program. Ca^{2+} signals are presented as F/F_o values or as $(F-F_{min})/(F_{max}-F)$, where F corresponds to the experimental fluorescence, F_o to the basal fluorescence, F_{max} to the fluorescence of Ca^{2+}-satured dye after addition of calcium ionophore ionomycin (100 μg/ml), and F_{min}, to the fluorescence signal obtained after Ca^{2+} chelation with BAPTA. In all cases, the increase in intracellular [Ca^{2+}] caused by AβOs did not saturate the probe, as indicated by the larger fluorescence increase caused by ionomycin. All experiments were done at room temperature (20–22°C).

Determination of mitochondrial fragmentation

Primary cultures, fixed with formaldehyde as described earlier, were immunolabeled with mouse anti-mHsp70 (1:750) by incubation for 1 h at room temperature. Cultures were rinsed 3 times with PBS and incubated for 1 h at room temperature with Alexa Fluor 488 anti-mouse as secondary antibody (1:400 in blocking solution). After three rinses with PBS, coverslips were mounted in DAKO mounting medium. Confocal image stacks were captured with a Zeiss LSM-5, Pascal 5 Axiovert 200 microscope, by using LSM 5 3.2 image capture and analysis software and a Plan-Apochromat 40×/1.4 Oil DIC objective. Image deconvolution was done with the Image J software, and z-stacks from images were reconstructed. The percentage of cells with a fragmented pattern was determined manually.

Additionally, we determined the association of the mitochondrial fission protein Drp-1 with mitochondria as a separate measure of enhanced mitochondrial fission. Mitochondrial extracts were prepared from 3 million cells for each condition, as previously described (51), and the content of Drp-1 present in these fractions was determined with Western blot analysis, as detailed later.

Determination of ATP cellular content

The CellTiter-GloTM luminescent assay kit (Promega, Madison, WI), based on ATP-dependent bioluminescence generation by luciferin/luciferase, was used to determine cellular ATP content. In brief, cells were seeded in a 96-well

plate at a density of 9×10^4 cells per well, and 45 μl of luminescent reagent (diluted 1:1 with PBS) was added to each well. After mixing and incubating for 10 min at room temperature, the ATP content was measured by using a Synergy 2 Biotek Model (Winooski, VT) plate reader.

Cytochrome c release

Cytochrome *c* release from mitochondria was detected with immunofluorescence by using confocal microscopy imaging. Cell cultures were fixed and immunostained for cytochrome *c*, as described earlier for other proteins. A punctate immunofluorescence indicates localization of cytochrome *c* to the mitochondria, whereas a diffuse pattern reflects cytochrome *c* release to the cytoplasm.

RNA isolation, PCR, and Western blot analysis

To extract RNA, cells were lysed as described in previous work (30). Total RNA was isolated by using Trizol reagent. To remove any contaminating genomic DNA, a DNAase digestion step with Ambion DNA-free Kit was included. RNA purity was assessed by the 260/280 absorbance ratio, and RNA integrity, with gel electrophoresis. cDNA was synthesized from total RNA (1 μg) by using the ImProm-II Reverse Transcriptase kit. Twenty-five nanograms of cDNA was used in 20-μl final volume for PCR amplification (Applied Biosystems Thermal cycler). Amplification was performed by using the primers and conditions detailed in Supplementary Table S1. Real-time quantitative PCR (qRT-PCR) was performed in an amplification system (MX3000P; Stratagene, La Jolla, CA) by using the DNA-binding dye SYBR green. Levels of RyR mRNA were calculated with the relative 2-ΔΔCt method (56), and normalized with respect to levels of β-actin mRNA. Dissociation curves were analyzed to verify the purity of products. All samples were run at least in triplicate.

For Western blot analysis of RyR2 and RyR3, cells extracts prepared as described (37) were resolved by SDS-PAGE (3.5–8% gradient or 10% polyacrylamide gels, transferred to PDVF membranes and incubated overnight with specific antibodies against RyR2 or RyR3). To correct for loading, membranes were stripped and probed for β-actin. Microsomes isolated from canine heart or rat brain cortex (9) were used as positive controls for RyR2 and RyR3, respectively. For Western blot analysis of Drp-1, proteins were resolved by SDS-PAGE (12% polyacrylamide gels), transferred to PDVF membranes, and incubated overnight with specific antibodies against Drp-1 (1:1,000). To correct for loading, membranes were stripped and probed against the specific mitochondrial marker enzyme COX IV (1:1,000). The Scion Image USI program (National Institutes of Health) was used to quantify optical band density.

Analysis of dendritic spine morphology changes

Hippocampal cultures (21 DIV) were loaded for 20 min with 1 μM calcein-AM in Tyrode solution. Confocal fluorescence and optical differential interference contrast (DIC) images were obtained with a Zeiss LSM-5, Pascal 5 Axiovert 200 microscope, by using LSM 5 3.2 image capture and analysis software and a Plan-Apochromat 63×/1.4 Oil DIC objective. We used the ImageJ software program (National Institutes of Health) for image deconvolution and generation of zeta projections from seven to 15 stacks (each 0.4-μm thickness). The 3D images were used simultaneously to identify and measure individual spines. To measure spine length, all spines in a single image plane were measured. Spine density in dendrites was analyzed by determining the number of spines present in a length of 100 μm; three to five dendrites were analyzed per condition in three independent experiments.

Statistics

Results are expressed as mean ± SEM. Unless otherwise indicated, statistical significance was evaluated by using the Student *t* test for paired data, and one-way or two-way ANOVA followed by Bonferroni's posttest for multiple determinations.

Results

Incubation of cultures for 6 h with 500 nM AβOs did not affect neuronal viability, assayed by Live/Dead cell staining, whereas incubation with 20 μM Aβ fibrils was highly toxic (Supplementary Fig. S2C), as previously described (54). Moreover, even 24-h incubation with 500 nM AβOs did not increase neuronal death, assayed with the MTT method (Supplementary Fig. S2D), confirming that 500 nM AβOs is a sublethal concentration (14). In contrast, 24-h incubation with AβOs at concentrations $\geq 1\ \mu M$ was significantly toxic to neurons, as was incubation with 50 μM *N*-methyl-D-aspartate (NMDA) or 50 μM glutamate used as positive controls of toxicity, which killed about 50% of neurons after 24 h of incubation (Supplementary Fig. S2D). Preincubation of cultures for 1 h with ryanodine (50 μM) did not protect against the enhanced neuronal death caused by subsequent incubation for 24 h with 1 μM AβOs, 50 μM NMDA, or 50 μM glutamate in the continuous presence of ryanodine, which by itself did not affect neuronal viability (Supplementary Fig. S2E). These results suggest that factors other than RyR-mediated Ca^{2+} release contribute to the neurotoxic effects of 1 μM AβOs, 50 μM NMDA, or 50 μM glutamate.

AβOs generate RyR-dependent Ca^{2+} signals

Addition of 500 nM AβOs, which, as shown earlier, is within the sublethal concentration range, produced a rapid and sizable increase in neuronal cytoplasmic free [Ca^{2+}], measured with the fluorescent Ca^{2+} indicator Fluo4-AM. As illustrated by a representative average fluorescence trace recorded from the soma of pyramidal neurons (Fig. 1A), this [Ca^{2+}] increase lasted several minutes before slowly decaying back to resting levels; in this experiment, the addition of AβOs produced maximum values of $(F-F_{min})/(F_{max}-F) = 2.09$ 0.13 (mean ± SEM, $n = 5$). The increase in intracellular [Ca^{2+}] caused by AβOs, which was consistently observed in 13 independent cultures, was suppressed by 1-h preincubation with 50 μM ryanodine added as a selective inhibitor of RyR-mediated Ca^{2+} release (Fig. 1B). Partial neuronal depolarization by addition of 20 mM KCl to primary cultures treated with AβOs (Fig. 1B inset, arrow) or to cultures preincubated with ryanodine and treated with AβOs (Fig. 1B, arrow) produced a small but significant [Ca^{2+}] increase in pyramidal cell soma, showing that ryanodine did not affect voltage-gated Ca^{2+} channels. Preincubation for 30 min with 10 μM MK-801 to inhibit NMDA receptors (NMDARs) also suppressed the Ca^{2+} increase induced by AβOs (Fig. 1C), as did removal of

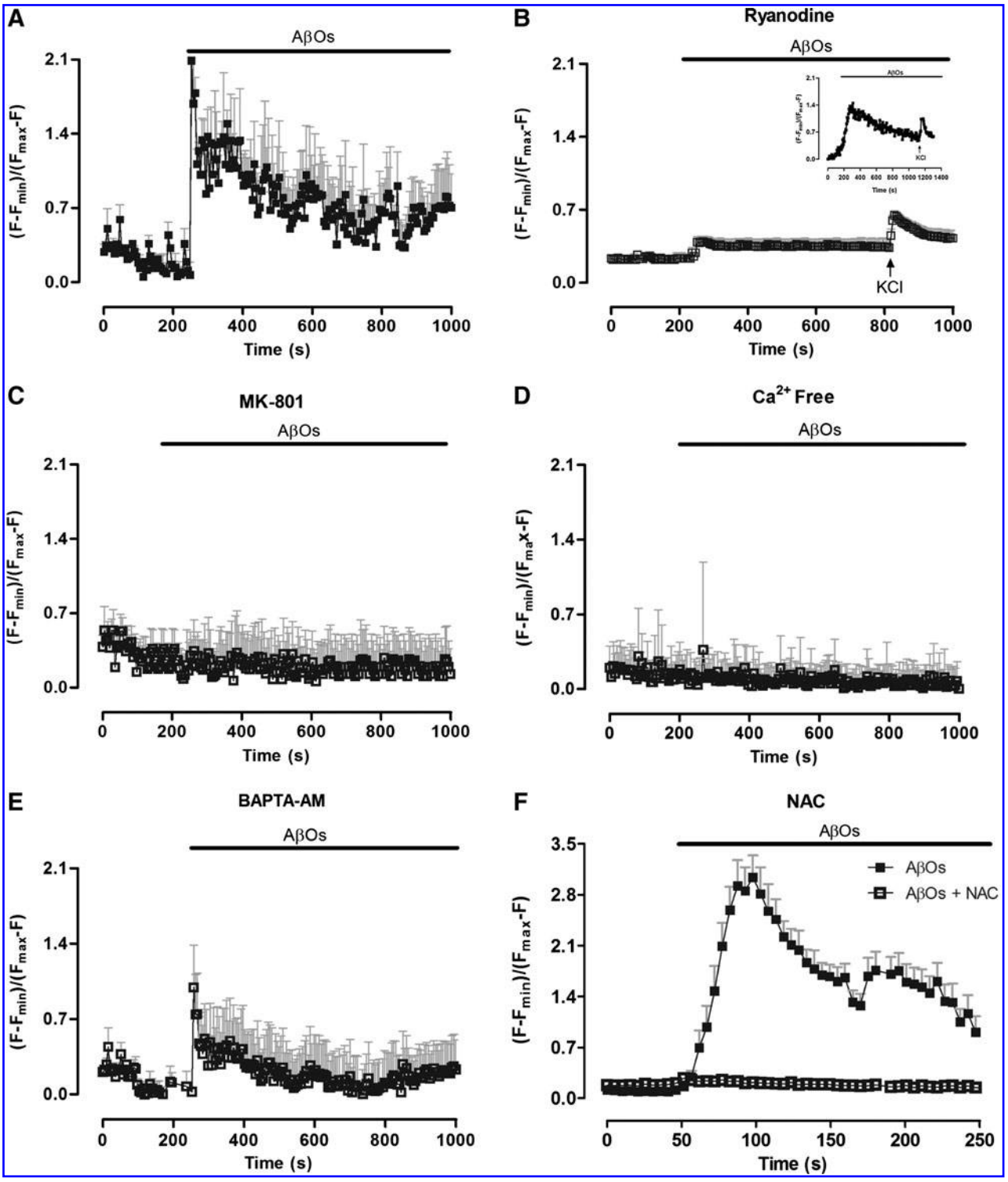

FIG. 1. Ca^{2+} signals elicited by Aβ Os require functional RyR. (A) Representative time course of Fluo4 fluorescence changes recorded before and after addition of Aβ Os (500 n*M*). **(B)** Inhibition of RyR-mediated Ca^{2+} release by preincubation with ryanodine (1 h, 50 μM) practically abolished Aβ Os-induced Ca^{2+} signals. Subsequent addition of 20 m*M* KCl (*arrow*) elicited a transient Ca^{2+} signal similar to that elicited by addition of 20 m*M* KCl to cultures treated with 500 n*M* Aβ Os (*inset*). Inhibition of NMDAR by preincubation for 30 min with 10 μM MK-801 **(C),** or incubation in Ca^{2+}-free solution **(D),** abolished Aβ Os-induced Ca^{2+} signals. **(E)** Preincubation for 30 min with 100 μM BAPTA-AM to chelate intracellular Ca^{2+} also suppressed, after some delay, the initial fluorescence increase caused by Aβ Os. **(F)** Preincubation for 1 h with 10 m*M* NAC to scavenge intracellular ROS also suppressed Aβ Os-induced Ca^{2+} signals. All fluorescence time-course data correspond to representative images of Fluo4 fluorescence (mean ± SEM) collected from the soma of five to seven pyramidal neurons. Similar findings were obtained in several ($n \geq 3$) independent hippocampal cultures.

external Ca^{2+}(Fig. 1D). Preincubation for 30 min with 100 μM BAPTA-AM to chelate intracellular Ca^{2+} also suppressed, after some delay, the initial increase in intracellular [Ca^{2+}] caused by AβOs (Fig. 1E), whereas preincubation with 10 m*M* *N*-acetyl-L-cysteine (NAC) for 1 h abolished the [Ca^{2+}] increase produced by AβOs (Fig. 1F).

To verify the effectiveness of 50 μM ryanodine in suppressing RyR-mediated Ca^{2+} release activity, we added 1 m*M* 4-cloro-methyl-cresol (4-CMC) to cultures loaded with Fluo4-AM. This RyR agonist produced a sizeable and sustained [Ca^{2+}] increase in the soma of control neurons but not in neurons preincubated with ryanodine, which did respond, however, to subsequent addition of 20 m*M* KCl (Supplementary Fig. S3A). Moreover, both control neurons and neurons preincubated with 50 μM ryanodine displayed a similar fluorescence increase after addition of 20 m*M* KCl, but the signal lasted significantly longer in control neurons (Supplementary Fig. S3B). These results show that that 50 μM ryanodine did not impair depolarization-induced Ca^{2+} entry but prevented the sustained phase of this response, suggesting that this delayed response takes place via RyR-mediated CICR. In addition, the stimulation of RyR-mediated Ca^{2+} release by 4-CMC was completely prevented by preincubation of primary cultures with 10 m*M* NAC for 60 min (Supplementary Fig. S3C). These results confirm that reducing agents prevent agonist-induced RyR activation in neurons (10).

Altogether, these results strongly suggest that stimulation of NMDAR-dependent Ca^{2+} entry by AβOs triggers RyR-mediated CICR in the oxidative intracellular environment produced by AβOs, which originates the persistent cytoplasmic [Ca^{2+}] increase observed after AβOs addition.

RyR inhibition prevents the neuronal mitochondrial fragmentation induced by AβOs

Confocal microscopy analysis revealed that 97% of primary hippocampal neurons contain elongated tubular mitochondria, exhibiting filamentous morphology of variable length in neuronal projections and the cell body (Fig. 2A). In contrast, 55% of neurons treated for 24 h with AβOs (500 n*M*) exhibited mitochondria with punctate morphology, revealing significant fragmentation of filamentous mitochondria (Fig. 2B). Incubation of cultures with 50 μM ryanodine for 4 h previous to AβOs addition significantly reduced (from 55% to 14%) the fraction of neurons exhibiting fragmented mitochondria (Fig. 2C), whereas neurons in cultures incubated with 50 μM ryanodine in the absence of AβOs had a content (97%) of elongated mitochondrial networks similar to that of controls (Fig. 2D).

Incubation of primary hippocampal cultures for only 6 h with 500 n*M* AβOs also induced noticeable mitochondrial fragmentation (data not shown), whereas incubation for 24 h with 1 μM AβOs, which decreased cell viability (Supplementary Fig. S2), produced even more mitochondrial fragmentation than did incubation with 500 n*M* AβOs for 24 h (data not shown).

To confirm that AβOs stimulated mitochondrial fragmentation, we detected in immunoblots the content of the fission protein Drp-1 in mitochondrial-enriched fractions isolated from control cultures of from cultures incubated with 500 n*M* AβOs for 24 h. As illustrated in Fig. 2E, Drp-1 was highly enriched in the mitochondrial fraction isolated from cultures incubated with AβOs compared with the controls. Furthermore, this sublethal concentration of AβOs did not impair mitochondrial ATP production or cause cytochrome *c* release (Supplementary Fig. S4). These results indicate that the mitochondrial fragmentation induced by AβOs did not produce substantial mitochondrial damage.

These combined results suggest that RyR-mediated Ca^{2+} release plays a major role in the mitochondrial network fragmentation induced by sublethal concentrations of AβOs.

AβOs downregulate RyR expression

Our observations suggest that RyR-mediated Ca^{2+} release is an early event triggered by AβOs. To define the possible impact of AβOs on RyR regulation, we examined RyR expression and localization in cells exposed to sublethal concentrations of AβOs. Immunofluorescence experiments revealed that incubation with 500 n*M* AβOs for 6 h, but not for 24 h, decreased the RyR2 protein content in both cell soma and neurites (Fig. 3), whereas RyR3 protein levels were not affected (data not shown). In agreement with these results, incubation with AβOs (500 n*M*) significantly decreased RyR2 mRNA levels after 6 h, and RyR3 mRNA after 12 h, and these levels remained reduced for up to 24 h (Fig. 4A). Western blot analysis revealed that AβOs also significantly reduced RyR2 protein content to 33% ($\pm$11%) of control after 1 h and to 44% ($\pm$3%) after 6 h ($n = 12$). Interestingly, these effects were transient, as RyR2 protein content was 113% ($\pm$6%) and 112% ($\pm$14%) of control after 12 h and 24 h of incubation with AβOs, respectively (Fig. 4B). In contrast, except for the small increase observed after 24 h, incubation with AβOs did not produce significant changes in RyR3 protein content (Fig. 4B). The RyR1 isoform was not detected in immunoblots when using antibodies that readily detect RyR1 in skeletal muscle microsomes (data not shown).

Ryanodine addition (50 μM) to cultures 1 h before AβOs provided significant, albeit partial, protection against the reduction of RyR2 protein content caused by incubation with 500 n*M* AβOs for 6 h (Fig. 5A). Preincubation with the

FIG. 2. AβOs induce mitochondrial network fragmentation: effects of RyR inhibition. (A) Confocal microscopy images of pyramidal neurons labeled with anti-mHSP70 antibody reveal normal filamentous mitochondrial network in control neurons. **(B)** This morphology contrasts with the fragmented pattern observed in neurons incubated with 500 nM AβOs for 24 h. **(C)** Inhibition of RyR-mediated Ca^{2+} release by preincubation with ryanodine (50 μM, 1 h) significantly prevented the mitochondrial fragmentation produced by AβOs. **(D)** RyR inhibition with ryanodine did not induce mitochondrial fragmentation by itself. Scale bar, 10 μm. **(E)** Quantification of the fraction of neurons exhibiting fragmented mitochondrial networks. Data are given as mean $\pm$ SEM. For further details, see text. **(F)** Changes in the levels of Drp-1 protein expression, normalized to β-actin. Results are expressed as mean $\pm$ SEM ($n = 4$). A representative Western blot showing Drp-1 content in mitochondria-enriched fractions extracted from neurons treated with AβOs (500 n*M*, 24 h) or neurons preincubated with ryanodine (50 μM, 1 h) is presented on top of the graph. Statistical significance was analyzed with ANOVA and the Bonferroni posttest. $^{***}p < 0.001$ relative to control. $^{\#\#}p < 0.01$ and $^{\#\#\#}p < 0.001$ relative to neurons treated with AβOs.

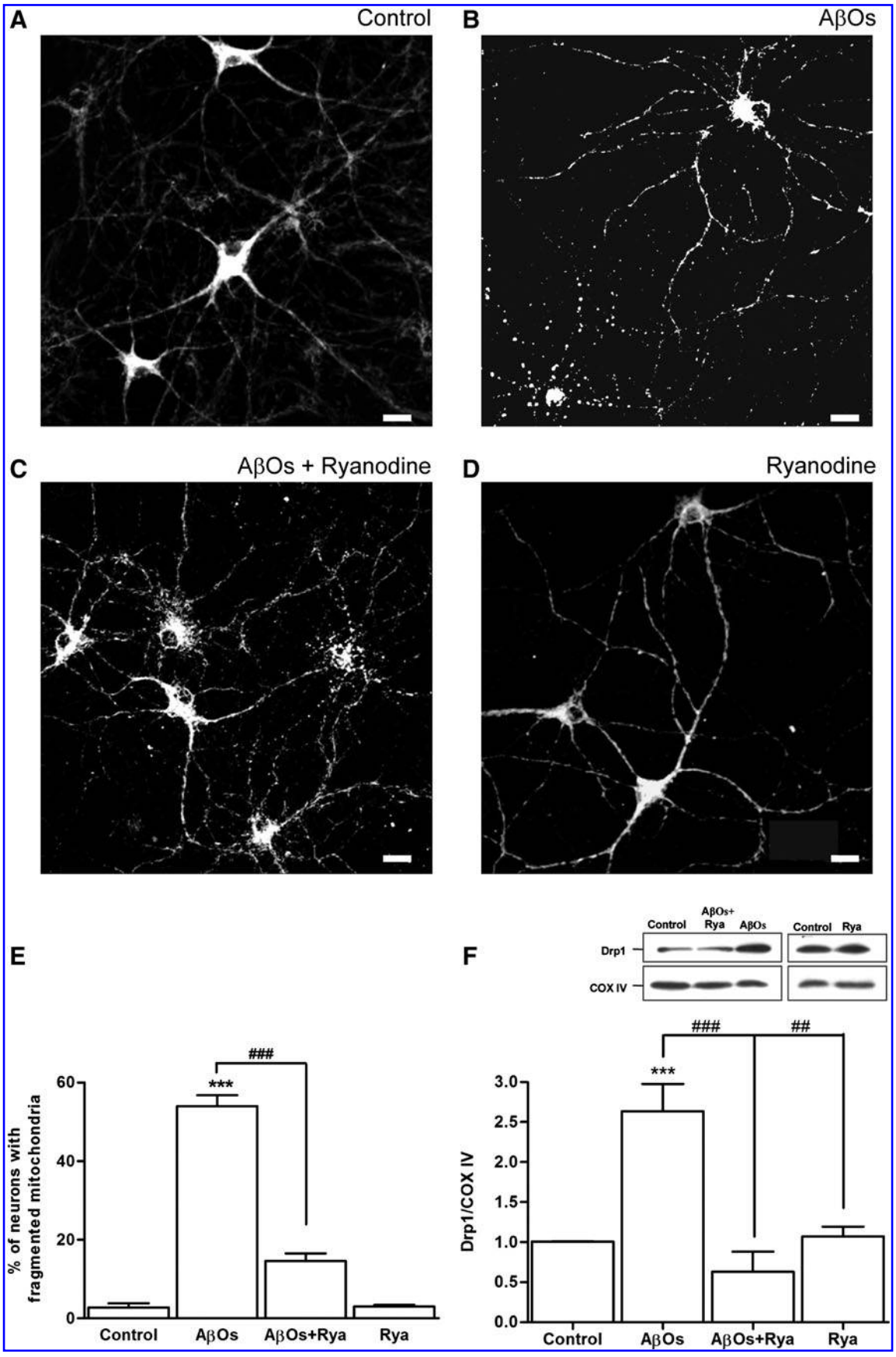
A
Control
B
AβOs
C
AβOs + Ryanodine
D
Ryanodine
E
% of neurons with fragmented mitochondria
60
40
20
0
***
###
Control
AβOs
AβOs+Rya
Rya
F
Control
AβOs+ Rya
AβOs
Control
Rya
Drp1
COX IV
Drp1/COX IV
3.0
2.5
2.0
1.5
1.0
0.5
0.0
***
###
##
Control
AβOs
AβOs+Rya
Rya

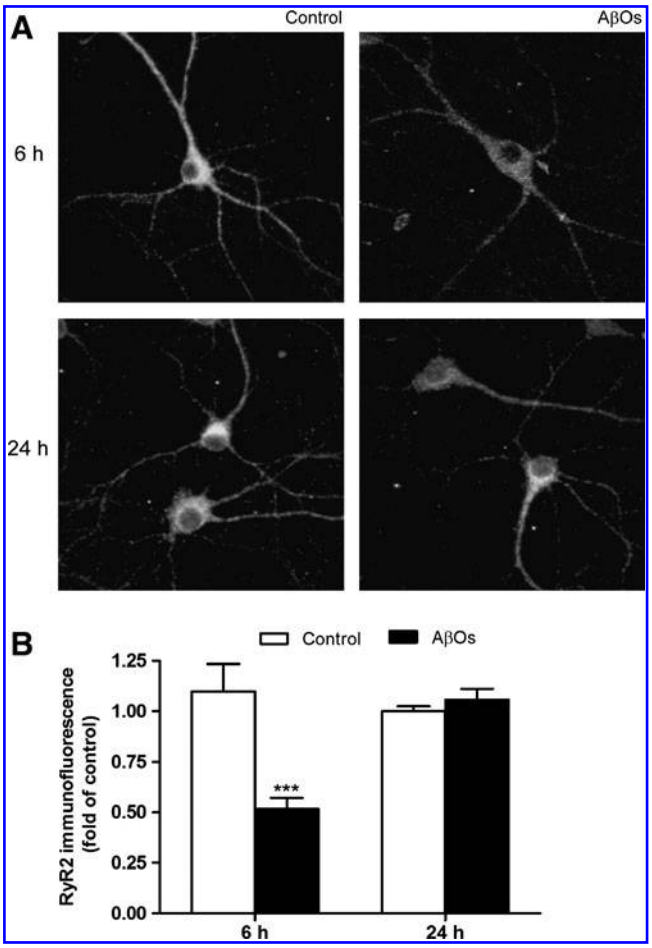

FIG. 3. AβOs decrease RyR2 protein content, as detected with immunofluorescence. Confocal microscopy images of pyramidal neurons labeled with anti-RyR2. **(A)** Hippocampal neurons were immunostained for RyR2, as described in the text. Representative images of control cultures or of cultures incubated with 500 n*M* AβOs for 6 or 24 h are presented. **(B)** Quantification of RyR2 immunofluorescence after incubation for 6 or 24 h with 500 n*M* AβOs ($n = 3$). Statistical significance was analyzed with ANOVA and the Bonferroni posttest. Data represent mean ± SEM. ***$p < 0.001$.

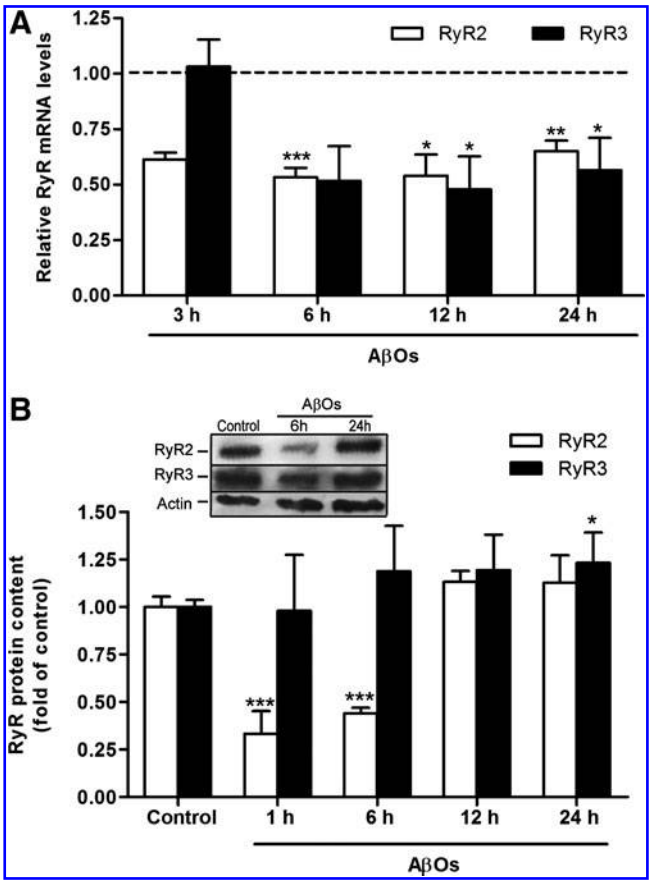

FIG. 4. AβOs downregulate RyR expression. (A) Time course of the changes induced by 500 n*M* AβOs in the levels of RyR2 and RyR3 mRNA determined with qRT-PCR (see text). All values were normalized to β-actin mRNA levels and expressed as fold of control. Values represent mean ± SEM of four different experiments, performed in triplicate. The error between controls in each experiment was <0.25. Statistical analysis was performed with the one-sample *t* test comparing column data against the hypothetical value of 1. *$p < 0.05$; **$p < 0.01$; and ***$p < 0.001$. **(B)** Representative Western blots for RyR2 and RyR3 in neurons treated with 500 n*M* AβOs for 6 or 24 h. Quantitative analysis of the time-course changes in the levels of RyR2 and RyR3 protein expression induced by AβOs, normalized to β-actin. Results are expressed as mean ± SEM ($n \geq 3$). Statistical significance was analyzed with ANOVA and the Bonferroni posttest. *$p < 0.05$; ***$p < 0.001$.

NMDAR inhibitor MK-801 (10 μM) completely abolished the reduction of RyR2 protein promoted by subsequent addition of AβOs (Fig. 5B). These results show that functional NMDAR and RyR-mediated Ca^{2+} signals participate in the cellular pathways that cause downregulation of RyR2 by AβOs.

AβOs prevent increased RyR2 expression and dendritic spine remodeling induced by BDNF

Preincubation of primary cultures for 1 h with 200 n*M* AβOs completely prevented the increase in RyR2 mRNA levels (Fig. 6A) and protein content (Fig. 6B) produced by subsequent incubation with BDNF (50 ng/ml) for 6 h. In addition, neurons incubated with BDNF for 6 h displayed a significant increase in spine density compared with the controls (Fig. 7A). Quantification of net changes revealed that BDNF increased spine density to values 1.4 ± 0.11 higher than controls (Fig. 7B). Addition of 500 n*M* AβOs 1 h before BDNF addition produced a drastic decrease in spine density (Fig. 7A) that reached values of 0.65 ± 0.1 compared with control neurons (Fig. 7B).

Addition of BDNF produced within minutes a significant increase in the length of preexistent spines (Fig. 7C, solid circles) and prompted the formation of new spines in control neurons, as illustrated by the images shown at the right, taken 60 min after BDNF addition. This spine remodeling did not occur after addition of BDNF to neurons preincubated with 500 n*M* AβOs for 6 h (Fig. 7C, solid squares). In contrast, neurons preincubated with 500 n*M* AβOs for 24 h displayed significant increases in spine length after the addition of BDNF (Fig. 7C, solid triangles), albeit at a slower rate than that displayed by control neurons after BDNF addition. Control neurons incubated with caffeine (10 m*M*), a well-known RyR

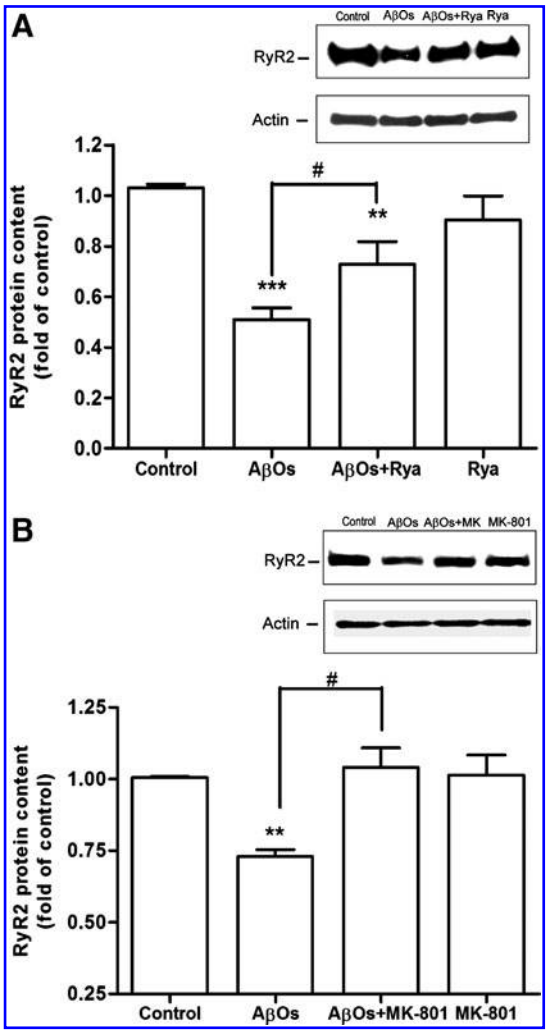

FIG. 5. MK-801 and ryanodine reverse RyR2 down-regulation induced by AβOs. Representative Western blots for RyR2 and quantitative analysis of the levels of RyR2 protein expression, normalized to β-actin, in neurons pre-incubated with **(A)** 50 μ*M* ryanodine or **(B)** 10 μ*M* MK-801, and subsequently incubated for 6 h with 500 n*M* AβOs. Results are expressed as mean ± SEM of three to five independent experiments. Statistical significance was analyzed with ANOVA and the Bonferroni posttest.*$p < 0.05$; **$p < 0.01$; and ***$p < 0.001$ in reference to the control. #$p < 0.05$ indicates significant difference from the condition indicated in the figure.

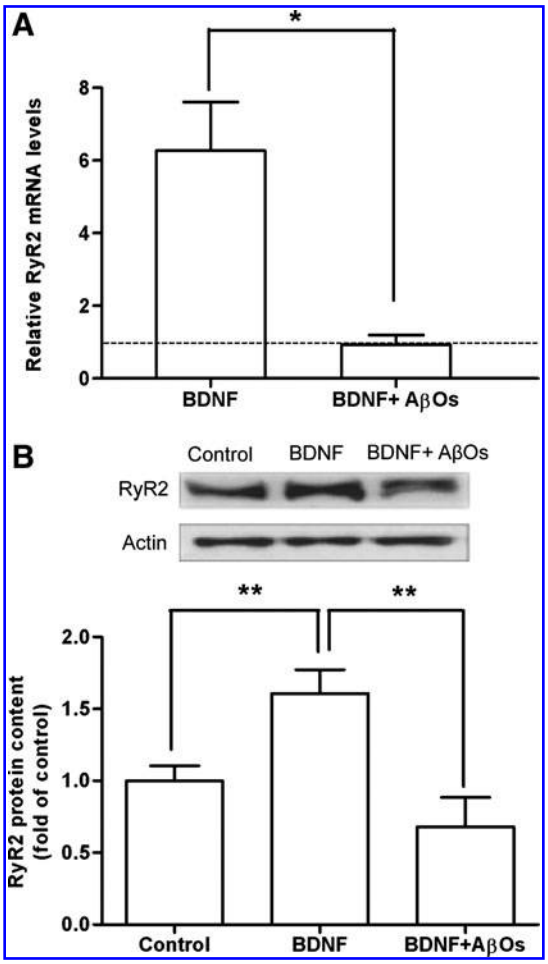

FIG. 6. AβOs prevent BDNF-induced increases in RyR2 expression. Hippocampal cultures were preincubated with 200 n*M* AβOs or vehicle for 1 h before incubation for 6 h with BDNF (50 ng/ml). **(A)** Relative RyR2 mRNA levels were determined with qRT-PCR, and normalized to β-actin mRNA levels. Results were evaluated with the Student *t* test. *$p < 0.05$. **(B)** Representative Western blot showing RyR2 and β-actin (*top*), and quantification of the relative RyR2 protein content respect to β-actin (*bottom*). Results are expressed as mean ± SEM of four separate experiments. Statistical significance was analyzed with one-way ANOVA followed by the Bonferroni multiple-comparison test. **$p < 0.01$.

agonist that promotes RyR-dependent spine growth (39), also exhibited significant spine elongation 45 min after caffeine addition (Fig. 7D, solid circles). Significantly, preincubation with AβOs (500 n*M*) for 6 h abolished the spine-length increases induced by caffeine (Fig. 7D, solid squares).

On the whole, these combined results suggest that inhibition of BDNF-induced RyR expression and spine remodeling may contribute to the synaptic plasticity defects induced by AβOs.

Discussion

The results presented here show for the first time that exposure of primary hippocampal neurons to sublethal concentrations of AβOs, the synaptotoxic soluble Aβ aggregates implicated in AD pathology, generated RyR-mediated Ca^{2+} signals within seconds in control neurons. These signals did not occur in neurons treated with MK-801, ryanodine, or NAC or in neurons bathed in Ca^{2+}-free solution, implicating Ca^{2+} entry via NMDAR and RyR-mediated CICR in their generation. Within a few hours, AβOs also produced a transient decrease in RyR2 protein expression and prevented the RyR2-expression enhancement and spine-morphology changes induced by BDNF. Longer treatment with AβOs (24 h) induced mitochondrial fission, which was significantly decreased by RyR inhibition.

RyR-mediated Ca^{2+} signals

Previous reports indicate that the fast generation of Ca^{2+} signals by AβOs requires extracellular Ca^{2+} (17) and

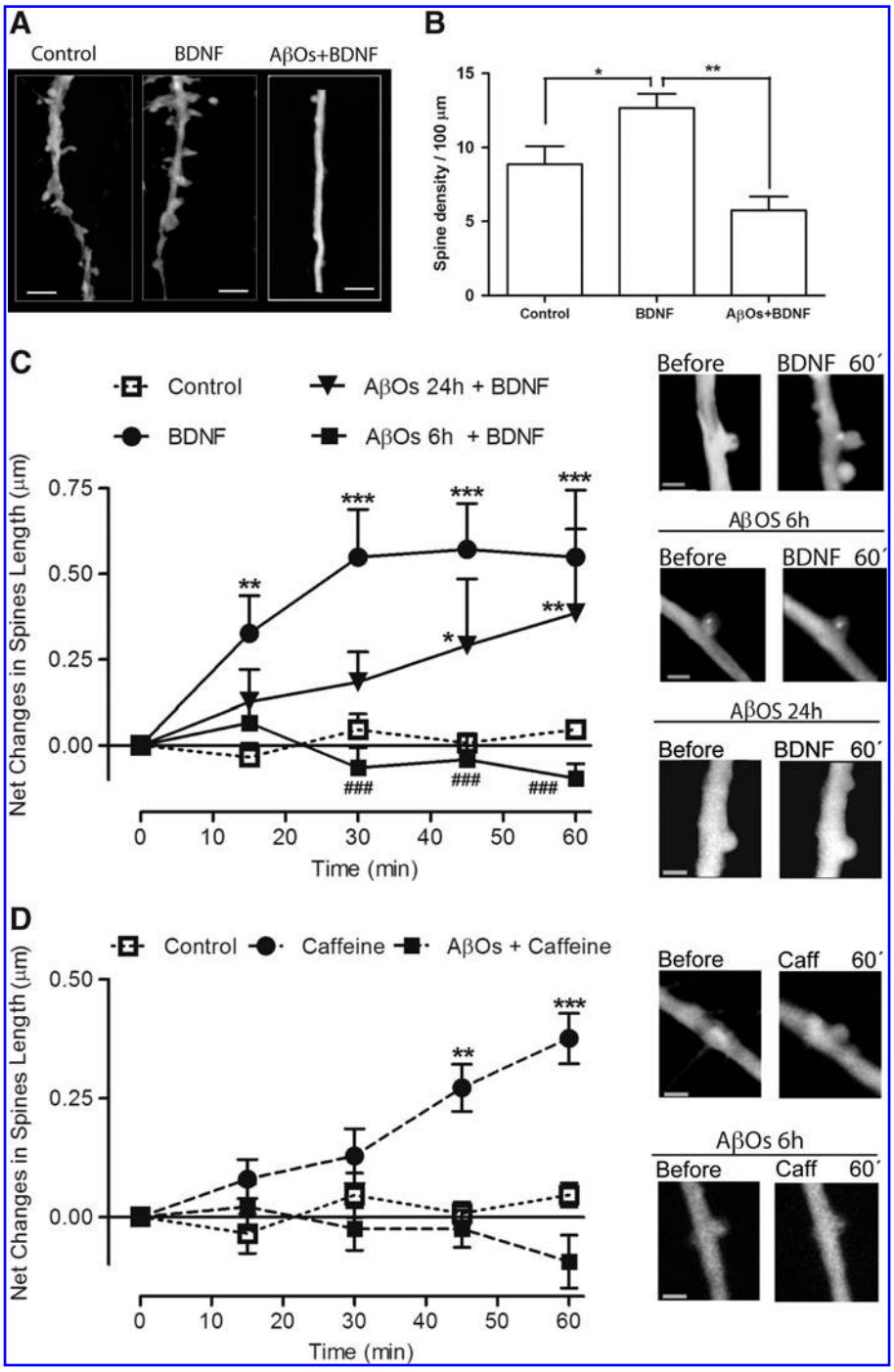

FIG. 7. AβOs prevent BDNF-induced changes in spine morphology and density. Hippocampal neurons loaded with calcein were visualized with confocal microscopy. **(A)** Representative images of dendritic spines in control neurons, in neurons exposed to BDNF for 6 h, and in neurons preincubated with 500 n*M* Aβ*O*s for 1 h before loading with calcein and subsequently treated with BDNF (50 ng/ml). Scale bar, 5 μm. **(B)** Quantification of changes in spine density. Results represent mean ± SEM ($n = 3$–6). Statistical significance was analyzed with one-way ANOVA, followed by the Bonferroni posttest. $^{*}p < 0.05$; $^{**}p < 0.01$. **(C)** *Left*: Quantification of net changes in spine length in control neurons (empty squares, $n = 8$), in neurons exposed to 50 ng/ml BDNF (solid circles, $n = 10$), and in neurons preincubated with 500 n*M* Aβ*O*s for 6 h (solid squares, $n = 4$) or for 24 h (solid triangles, $n = 13$) before calcein loading and before addition of BDNF. Results represent mean ± SEM. Statistical significance was analyzed with two-way ANOVA, followed by the Bonferroni posttest. $^{*}p < 0.05$; $^{**}p < 0.01$; $^{***}p < 0.001$, statistically significantly different from control; $^{\#\#\#}p < 0.001$ relative to BDNF-treated neurons. *Right*: Fluorescent confocal images of a neurite from a neuron stimulated for 60 min with BDNF (50 ng/ml); spine elongation and formation of a new spine can be appreciated. Incubation with 500 n*M* Aβ*O*s for 6 h before calcein loading prevented the dendritic-spine changes induced by BDNF, whereas spines from neurons preincubated with 500 n*M* Aβ*O*s for 24 h displayed slower but significant increases in length after addition of BDNF. Scale bar, 2 μm. **(D)** *Left*: Quantification of net changes in spine length in control neurons (open squares, $n = 8$), in neurons exposed to 10 m*M* caffeine (solid circles, $n = 25$), and in neurons preincubated with 500 n*M* Aβ*O*s for 6 h (solid squares, $n = 23$) before calcein loading and subsequent addition of BDNF. Results represent mean ± SEM. Statistical significance was analyzed with two-way ANOVA, followed by the Bonferroni posttest. $^{**}p < 0.01$; $^{***}p < 0.001$, statistically significant difference from control. *Right*: Fluorescent confocal images of a neurite from a neuron stimulated for 60 min with caffeine (10 m*M*); spine elongation is observed. Incubation with 500 n*M* Aβ*O*s for 6 h before calcein loading prevented the dendritic-spine changes induced by caffeine. Scale bar, 2 μm.

functional NMDAR (14). Adding to these previous studies, our findings indicate for the first time that RyR-mediated Ca^{2+} release is the primary source of the sustained Ca^{2+} signals generated by Aβ*O*s, because they were abolished by selective RyR inhibition. Our results strongly suggest that the stimulation of Ca^{2+} entry via NMDAR produced by Aβ*O*s does not generate substantial Ca^{2+} signals by itself but stimulates RyR via CICR, a well-known response of excitable cells to Ca^{2+} entry fluxes. In particular, we have shown that high-frequency field stimulation of primary hippocampal neurons

elicits RyR-mediated CICR that is prevented by preincubation with NAC (61). We report that preincubation with the general antioxidant NAC completely prevented the emergence of Ca^{2+} signals induced by AβOs. This finding agrees well with previous studies showing that reducing agents suppress Ca^{2+} activation of neuronal RyR at the single-channel level (10).

Ample consensus exists that Ca^{2+} signals, including signals generated by Ca^{2+} release from the ER (5), activate neuronal signaling cascades that play essential roles in synaptic plasticity and memory formation (28). Yet, prolonged increases in intracellular [Ca^{2+}], such as those produced by AβOs, produce harmful effects (26, 78). Moreover, Ca^{2+} released from the ER increases Aβ production and the Aβ42/40 ratio (12), and ER Ca^{2+} mishandling seems to contribute to synaptic dysfunctions in AD (7). Familial AD presenilin mutations impair the function of presenilins as ER Ca^{2+} leak channels, resulting in excessive ER Ca^{2+} accumulation that enhances Ca^{2+} release through RyR and IP3 receptor channels (47, 48, 70). Presenilins can also interact directly or indirectly with RyR and the sarco/endoplasmic reticulum Ca^{2+}-ATPase to alter ER Ca^{2+} release and uptake (8).

Our results indicate that RyR-mediated Ca^{2+} signals generated by AβOs contribute to the increased mitochondrial fission produced by long (24 h) incubation with AβOs, as RyR inhibition reduced significantly the mitochondrial fragmentation. A sustained increase in cytoplasmic [Ca^{2+}], such as that induced by AβOs, is likely to promote an increase in mitochondrial Ca^{2+}, a condition that promotes mitochondrial fragmentation (32, 34). It has been reported that AβOs (500 n*M*) increased within minutes the mitochondrial Ca^{2+} in cerebellar granule cells, whereas release of cytochrome *c* and apoptosis occurred only after 72 h of incubation with AβOs (62).

In rat primary hippocampal neurons, APP overexpression induces mitochondrial fragmentation, probably through increased Aβ peptide production (75), whereas treatment for 24 h with AβOs (800 n*M*) also produces loss of dendritic spines, in addition to mitochondrial fragmentation (74). These combined reports, plus our own results, suggest that increased mitochondrial fission, likely due to mitochondrial Ca^{2+} overload produced by the prolonged RyR-mediated Ca^{2+} signals generated by AβOs, may contribute to mitochondrial and neuronal dysfunction in AD brain.

RyR expression

Hippocampal neurons express RyR in axons, dendrites, and dendritic spines, whereas IP3 receptors are expressed throughout hippocampal cells but not in dendritic spines (64). Our results indicate that the RyR2 and RyR3 isoforms are abundantly present in cell bodies and neurites of primary hippocampal neurons. In addition, we show that incubation with AβOs for 6 h produced a transient decrease in RyR2 protein expression in these neurons without affecting RyR3.

Our results showing decreased RyR2 expression in neurons treated with AβOs, even after treatment with BDNF, agree well with a previous report describing that AD human cortex displays reduced RyR2 protein content and decreased [^{3}H]-ryanodine binding, a likely consequence of decreased RyR2 content (36). Given the prominent role played by RyR-mediated Ca^{2+} signals in synaptic transmission and neuronal plasticity (4, 19, 22, 33, 39, 45), a decrease in RyR2 expression may contribute to the defective synaptic plasticity produced by AβOs. Moreover, hippocampal expression of the RyR2 isoform increases after spatial memory training (77), and selective RyR2 and RyR3 knockdown with antisense oligonucleotides impairs memory processes (22). Accordingly, by transiently decreasing RyR2 expression, among other effects, AβOs may impair hippocampal memory formation.

Our *in silico* analysis revealed that the published rat RyR2 gene sequence contains response elements to the Ca^{2+}-activated transcriptional regulators CREB and NFAT. These regulators may respond to RyR-mediated Ca^{2+} signals induced by AβOs, generating changes in expression of RyR2 and other proteins. The finding that RyR inhibition partially protected against the decrease in RyR2 expression produced by AβOs supports the involvement of RyR-mediated Ca^{2+} signals in this decrease. It is worth mentioning in this context that tissue from AD brains displays significant downregulation of neuronal calcineurin (11), a Ca^{2+}-activated phosphatase known to play fundamental roles in synaptic plasticity and long-term depression (LTD). Yet, incubation of human SY5Y neuroblastoma cells with AβOs for 3 h significantly increases calcineurin activity, leading to decreased CREB phosphorylation and CREB-driven transcriptional activity (59). Moreover, calcineurin and AβOs jointly decrease CREB phosphorylation (68). A decrease in CREB phosphorylation may underlie the reduction in RyR2 expression produced by AβOs, even after BDNF addition. Future studies should address how prolonged RyR-mediated Ca^{2+} signals induced by AβOs, which can be prevented by inhibition of NMDAR activity, stimulate pathways that downregulate hippocampal RyR2 expression, and should also address whether these signals contribute to activate calcineurin-mediated LTD during the progression of AD.

Synaptic spine remodeling

Hippocampal synaptic plasticity requires significant postsynaptic remodeling, which entails the generation and growth of dendritic spines (38). Significantly, incubation with AβOs for a period of 6 h prevented the rapid spine remodeling prompted by caffeine-induced RyR-mediated Ca^{2+} release (39) or by BDNF, which also requires RyR-mediated Ca^{2+} signals (1). These results strongly suggest that the transient RyR2 decrease induced by AβOs (6 h) produces a significant reduction of RyR2-mediated Ca^{2+} signals in response to BDNF, leading to defective synaptic remodeling in primary hippocampal neurons. In contrast, RyR2 expression and BDNF-induced spine remodeling were similar to the controls after longer incubation (24 h) with AβOs. These findings suggest that primary hippocampal neurons possess mechanisms to compensate for the significant short-term loss of RyR2 produced by AβOs. Moreover, incubation with AβOs for 24 h produced a small (23%) but significant increase in RyR3 protein content, which may contribute to producing the Ca^{2+} signals that underlie BDNF-induced spine remodeling.

Previous reports indicate that AβOs downregulate BDNF expression (55) and interfere with BDNF-induced signaling pathways that include Ca^{2+}-dependent kinase pathways that enhance CREB phosphorylation (68). AβOs also decrease rapidly the NMDAR and EphB2 receptor expression in the plasma membrane, followed by the development of abnormal dendritic spine morphology and spine degeneration (41). These factors, plus the present findings showing that AβOs

transiently decreased RyR2 protein expression, prevented the RyR2-expression enhancement and spine-morphology changes induced by BDNF and induced mitochondrial fission, may act in conjunction to provoke the strong synaptotoxicity caused by AβOs.

Concluding Remarks

The hippocampus is a brain structure specifically associated with memory formation that is severely affected early in the course of AD (18). In normal brain, long-lasting synaptic plasticity (49) and hippocampal memory formation (2) require extensive synaptic spine remodeling, which is made possible by changes in gene transcription and the ensuing protein synthesis (6, 21, 76). The present results demonstrate that AβOs rapidly generated prolonged RyR-mediated Ca^{2+} signals. We propose that, by engaging Ca^{2+}-dependent pathways, these signals may cause the observed decrease in RyR2 expression that presumably contributes to suppress the RyR-dependent spine growth induced by BDNF. Downregulation of RyR2 expression, which occurred even in neurons treated with BDNF, in addition to the partly RyR-dependent mitochondrial fragmentation caused by AβOs, may contribute to produce the hippocampal synaptotoxicity and defective synaptic plasticity induced by soluble Aβ oligomers in AD.

Acknowledgments

This work was supported by Fondecyt postdoctoral project 3085025 and by CONICYT-FONDAP 79090021 to A.C. Paula-Lima, by Fondecyt grants 1060177 and 1100176, and by Fondecyt-FONDAP 15010006. C. Hetz also acknowledges support from Millennium Nucleus P07-048-F and CHDI-HighQ Foundation, and S. T. Ferreira from Conselho Nacional de Desenvolvimento Cientifico e Tecnológico, Fundacao de Amparo à Pesquisa do Estado do Rio de Janeiro and Instituto Nacional de Neurociência Translacional. The authors gratefully acknowledge Drs. J. Hidalgo, P. Donoso and G. Sanchez for their thoughtful comments and support, and thank N. Leal and P. Fernández for their skilful professional assistance.

Author Disclosure Statement

No competing financial interests exist.

References

1. Adasme T, Paula-Lima A, Humeres A, Muñoz P, Olivero P, Leal N, Ferreira ST, Carrasco MA, and Hidalgo C. Changes in ryanodine receptor expression and activity in hippocampal neurons in primary culture exposed to BDNF or amyloid β peptide oligomers. Program N° 529.6/C36. 2008 Neuroscience Meeting Planner. Washington, DC: Society for Neuroscience 2008. Abstract available online.

1a. Alberdi E, Sanchez-Gomez MV, Cavaliere F, Perez-Samartin A, Zugaza JL, Trullas R, Domercq M, and Matute C. Amyloid beta oligomers induce Ca^{2+} dysregulation and neuronal death through activation of ionotropic glutamate receptors. *Cell Calcium* 47: 264–272, 2010.

2. Alberini CM. Transcription factors in long-term memory and synaptic plasticity. *Physiol Rev* 89: 121–145, 2009.

3. Alonso M, Medina JH, and Pozzo-Miller L. ERK1/2 activation is necessary for BDNF to increase dendritic spine density in hippocampal CA1 pyramidal neurons. *Learn Mem* 11: 172–178, 2004.

4. Balschun D, Wolfer DP, Bertocchini F, Barone V, Conti A, Zuschratter W, Missiaen L, Lipp HP, Frey JU, and Sorrentino V. Deletion of the ryanodine receptor type 3 (RyR3) impairs forms of synaptic plasticity and spatial learning. *EMBO J* 18: 5264–5273, 1999.

5. Bardo S, Cavazzini MG, and Emptage N. The role of the endoplasmic reticulum Ca2+ store in the plasticity of central neurons. *Trends Pharmacol Sci* 27: 78–84, 2006.

6. Barondes SH and Jarvik ME. The influence of actinomycin-D on brain RNA synthesis and on memory. *J Neurochem* 11: 187–195, 1964.

7. Berridge MJ. Calcium hypothesis of Alzheimer's disease. *Pflugers Arch* 459: 441–449, 2010.

8. Bezprozvanny I and Mattson MP. Neuronal calcium mishandling and the pathogenesis of Alzheimer's disease. *Trends Neurosci* 31: 454–463, 2008.

9. Bull R, Finkelstein JP, Galvez J, Sanchez G, Donoso P, Behrens MI, and Hidalgo C. Ischemia enhances activation by Ca2+ and redox modification of ryanodine receptor channels from rat brain cortex. *J Neurosci* 28: 9463–9472, 2008.

10. Bull R, Finkelstein JP, Humeres A, Behrens MI, and Hidalgo C. Effects of ATP, Mg2+, and redox agents on the Ca2+ dependence of RyR channels from rat brain cortex. *Am J Physiol Cell Physiol* 293: C162–C171, 2007.

11. Celsi F, Svedberg M, Unger C, Cotman CW, Carri MT, Ottersen OP, Nordberg A, and Torp R. Beta-amyloid causes downregulation of calcineurin in neurons through induction of oxidative stress. *Neurobiol Dis* 26: 342–352, 2007.

12. Cheung KH, Shineman D, Muller M, Cardenas C, Mei L, Yang J, Tomita T, Iwatsubo T, Lee VM, and Foskett JK. Mechanism of Ca2+ disruption in Alzheimer's disease by presenilin regulation of InsP3 receptor channel gating. *Neuron* 58: 871–883, 2008.

13. Danzer SC, Crooks KR, Lo DC, and McNamara JO. Increased expression of brain-derived neurotrophic factor induces formation of basal dendrites and axonal branching in dentate granule cells in hippocampal explant cultures. *J Neurosci* 22: 9754–9763, 2002.

14. De Felice FG, Velasco PT, Lambert MP, Viola K, Fernandez SJ, Ferreira ST, and Klein WL. Abeta oligomers induce neuronal oxidative stress through an N-methyl-D-aspartate receptor-dependent mechanism that is blocked by the Alzheimer drug memantine. *J Biol Chem* 282: 11590–11601, 2007.

15. De Felice FG, Vieira MN, Bomfim TR, Decker H, Velasco PT, Lambert MP, Viola KL, Zhao WQ, Ferreira ST, and Klein WL. Protection of synapses against Alzheimer's-linked toxins: insulin signaling prevents the pathogenic binding of Abeta oligomers. *Proc Natl Acad Sci U S A* 106: 1971–1976, 2009.

16. De Felice FG, Wu D, Lambert MP, Fernandez SJ, Velasco PT, Lacor PN, Bigio EH, Jerecic J, Acton PJ, Shughrue PJ, Chen-Dodson E, Kinney GG, and Klein WL. Alzheimer's disease-type neuronal tau hyperphosphorylation induced by A beta oligomers. *Neurobiol Aging* 29: 1334–1347, 2008.

17. Demuro A, Mina E, Kayed R, Milton SC, Parker I, and Glabe CG. Calcium dysregulation and membrane disruption as a ubiquitous neurotoxic mechanism of soluble amyloid oligomers. *J Biol Chem* 280: 17294–17300, 2005.

18. deToledo-Morrell L, Stoub TR, and Wang C. Hippocampal atrophy and disconnection in incipient and mild Alzheimer's disease. *Prog Brain Res* 163: 741–753, 2007.

19. Emptage N, Bliss TV, and Fine A. Single synaptic events evoke NMDA receptor-mediated release of calcium from

internal stores in hippocampal dendritic spines. *Neuron* 22: 115–124, 1999.
20. Ferreiro E, Resende R, Costa R, Oliveira CR, and Pereira CM. An endoplasmic-reticulum-specific apoptotic pathway is involved in prion and amyloid-beta peptides neurotoxicity. *Neurobiol Dis* 23: 669–678, 2006.
21. Flexner JB, Flexner LB, Stellar E, De La Haba G, and Roberts RB. Inhibition of protein synthesis in brain and learning and memory following puromycin. *J Neurochem* 9: 595–605, 1962.
22. Galeotti N, Quattrone A, Vivoli E, Norcini M, Bartolini A, and Ghelardini C. Different involvement of type 1, 2, and 3 ryanodine receptors in memory processes. *Learn Mem* 15: 315–323, 2008.
23. Garzon DJ and Fahnestock M. Oligomeric amyloid decreases basal levels of brain-derived neurotrophic factor (BDNF) mRNA via specific downregulation of BDNF transcripts IV and V in differentiated human neuroblastoma cells. *J Neurosci* 27: 2628–2635, 2007.
24. Giannini G, Conti A, Mammarella S, Scrobogna M, and Sorrentino V. The ryanodine receptor/calcium channel genes are widely and differentially expressed in murine brain and peripheral tissues. *J Cell Biol* 128: 893–904, 1995.
25. Giuffrida ML, Caraci F, Pignataro B, Cataldo S, De Bona P, Bruno V, Molinaro G, Pappalardo G, Messina A, Palmigiano A, Garozzo D, Nicoletti F, Rizzarelli E, and Copani A. Beta-amyloid monomers are neuroprotective. *J Neurosci* 29: 10582–10587, 2009.
26. Gleichmann M and Mattson MP. Neuronal calcium homeostasis and dysregulation. *Antioxid Redox Signal* 14: 1261–1273, 2011.
27. Glenner GG and Wong CW. Alzheimer's disease: initial report of the purification and characterization of a novel cerebrovascular amyloid protein. *Biochem Biophys Res Commun* 120: 885–890, 1984.
28. Greer PL and Greenberg ME. From synapse to nucleus: calcium-dependent gene transcription in the control of synapse development and function. *Neuron* 59: 846–860, 2008.
29. Haass C and Selkoe DJ. Soluble protein oligomers in neurodegeneration: lessons from the Alzheimer's amyloid beta-peptide. *Nat Rev Mol Cell Biol* 8: 101–112, 2007.
30. Haeger P, Alvarez A, Leal N, Adasme T, Nunez MT, and Hidalgo C. Increased hippocampal expression of the divalent metal transporter 1 (DMT1) mRNA variants 1B and +IRE and DMT1 protein after NMDA-receptor stimulation or spatial memory training. *Neurotox Res* 17: 238–247, 2010.
31. Hayrapetyan V, Rybalchenko V, Rybalchenko N, and Koulen P. The N-terminus of presenilin-2 increases single channel activity of brain ryanodine receptors through direct protein-protein interaction. *Cell Calcium* 44: 507–518, 2008.
32. Hom JR, Gewandter JS, Michael L, Sheu SS, and Yoon Y. Thapsigargin induces biphasic fragmentation of mitochondria through calcium-mediated mitochondrial fission and apoptosis. *J Cell Physiol* 212: 498–508, 2007.
33. Huddleston AT, Tang W, Takeshima H, Hamilton SL, and Klann E. Superoxide-induced potentiation in the hippocampus requires activation of ryanodine receptor type 3 and ERK. *J Neurophysiol* 99: 1565–1571, 2008.
34. Kaddour-Djebbar I, Choudhary V, Brooks C, Ghazaly T, Lakshmikanthan V, Dong Z, and Kumar MV. Specific mitochondrial calcium overload induces mitochondrial fission in prostate cancer cells. *Int J Oncol* 36: 1437–1444, 2010.
35. Kang H, Welcher AA, Shelton D, and Schuman EM. Neurotrophins and time: different roles for TrkB signaling in hippocampal long-term potentiation. *Neuron* 19: 653–664, 1997.
36. Kelliher M, Fastbom J, Cowburn RF, Bonkale W, Ohm TG, Ravid R, Sorrentino V, and O'Neill C. Alterations in the ryanodine receptor calcium release channel correlate with Alzheimer's disease neurofibrillary and beta-amyloid pathologies. *Neuroscience* 92: 499–513, 1999.
37. Kemmerling U, Munoz P, Muller M, Sanchez G, Aylwin ML, Klann E, Carrasco MA, and Hidalgo C. Calcium release by ryanodine receptors mediates hydrogen peroxide-induced activation of ERK and CREB phosphorylation in N2a cells and hippocampal neurons. *Cell Calcium* 41: 491–502, 2007.
38. Kitanishi T, Ikegaya Y, Matsuki N, and Yamada MK. Experience-dependent, rapid structural changes in hippocampal pyramidal cell spines. *Cereb Cortex* 19: 2572–2578, 2009.
39. Korkotian E and Segal M. Release of calcium from stores alters the morphology of dendritic spines in cultured hippocampal neurons. *Proc Natl Acad Sci U S A* 96: 12068–12072, 1999.
40. Kuczewski N, Porcher C, Lessmann V, Medina I, and Gaiarsa JL. Activity-dependent dendritic release of BDNF and biological consequences. *Mol Neurobiol* 39: 37–49, 2009.
41. Lacor PN, Buniel MC, Furlow PW, Clemente AS, Velasco PT, Wood M, Viola KL, and Klein WL. Abeta oligomer-induced aberrations in synapse composition, shape, and density provide a molecular basis for loss of connectivity in Alzheimer's disease. *J Neurosci* 27: 796–807, 2007.
42. Lambert MP, Barlow AK, Chromy BA, Edwards C, Freed R, Liosatos M, Morgan TE, Rozovsky I, Trommer B, Viola KL, Wals P, Zhang C, Finch CE, Krafft GA, and Klein WL. Diffusible, nonfibrillar ligands derived from Abeta1-42 are potent central nervous system neurotoxins. *Proc Natl Acad Sci U S A* 95: 6448–6453, 1998.
43. Li S, Hong S, Shepardson NE, Walsh DM, Shankar GM, and Selkoe D. Soluble oligomers of amyloid beta protein facilitate hippocampal long-term depression by disrupting neuronal glutamate uptake. *Neuron* 62: 788–801, 2009.
44. Lorenzo A and Yankner BA. Beta-amyloid neurotoxicity requires fibril formation and is inhibited by congo red. *Proc Natl Acad Sci U S A* 91: 12243–12247, 1994.
45. Lu YF and Hawkins RD. Ryanodine receptors contribute to cGMP-induced late-phase LTP and CREB phosphorylation in the hippocampus. *J Neurophysiol* 88: 1270–1278, 2002.
46. Masters CL, Simms G, Weinman NA, Multhaup G, McDonald BL, and Beyreuther K. Amyloid plaque core protein in Alzheimer disease and Down syndrome. *Proc Natl Acad Sci U S A* 82: 4245–4249, 1985.
47. Müller M, Cheung K-H and Foskett JK. Enhanced ROS generation mediated by Alzheimer's disease presenilin regulation of $InsP_3R$ Ca^{2+} signaling. *Antioxid Redox Signal* 14: 1225–1235, 2011.
48. Nelson O, Tu H, Lei T, Bentahir M, de Strooper B, and Bezprozvanny I. Familial Alzheimer disease-linked mutations specifically disrupt Ca2+ leak function of presenilin 1. *J Clin Invest* 117: 1230–1239, 2007.
49. Nguyen PV and Kandel ER. A macromolecular synthesis-dependent late phase of long-term potentiation requiring cAMP in the medial perforant pathway of rat hippocampal slices. *J Neurosci* 16: 3189–3198, 1996.
50. Orrenius S, Zhivotovsky B, and Nicotera P. Regulation of cell death: the calcium-apoptosis link. *Nat Rev Mol Cell Biol* 4: 552–565, 2003.
51. Parra V, Eisner V, Chiong M, Criollo A, Moraga F, Garcia A, Hartel S, Jaimovich E, Zorzano A, Hidalgo C, and Lavandero S. Changes in mitochondrial dynamics during ceramide-induced cardiomyocyte early apoptosis. *Cardiovasc Res* 77: 387–397, 2008.

52. Paula-Lima AC, De Felice FG, Brito-Moreira J, and Ferreira ST. Activation of GABA(A) receptors by taurine and muscimol blocks the neurotoxicity of beta-amyloid in rat hippocampal and cortical neurons. *Neuropharmacology* 49: 1140–1148, 2005.
53. Paula-Lima AC, De Felice FG, Brito-Moreira J, and Ferreira ST. Activation of GABA(A) receptors by taurine and muscimol blocks the neurotoxicity of beta-amyloid in rat hippocampal and cortical neurons. *Neuropharmacology* 49: 1140–1148, 2005.
54. Paula-Lima AC, Tricerri MA, Brito-Moreira J, Bomfim TR, Oliveira FF, Magdesian MH, Grinberg LT, Panizzutti R, and Ferreira ST. Human apolipoprotein A-I binds amyloid-beta and prevents Abeta-induced neurotoxicity. *Int J Biochem Cell Biol* 41: 1361–1370, 2009.
55. Peng S, Garzon DJ, Marchese M, Klein W, Ginsberg SD, Francis BM, Mount HT, Mufson EJ, Salehi A, and Fahnestock M. Decreased brain-derived neurotrophic factor depends on amyloid aggregation state in transgenic mouse models of Alzheimer's disease. *J Neurosci* 29: 9321–9329, 2009.
56. Pfaffl MW. A new mathematical model for relative quantification in real-time RT-PCR. *Nucleic Acids Res* 29: e45, 2001.
57. Pike CJ, Walencewicz AJ, Glabe CG, and Cotman CW. In vitro aging of beta-amyloid protein causes peptide aggregation and neurotoxicity. *Brain Res* 563: 311–314, 1991.
58. Poo MM. Neurotrophins as synaptic modulators. *Nat Rev Neurosci* 2: 24–32, 2001.
59. Reese LC, Zhang W, Dineley KT, Kayed R, and Taglialatela G. Selective induction of calcineurin activity and signaling by oligomeric amyloid beta. *Aging Cell* 7: 824–835, 2008.
60. Resende R, Ferreiro E, Pereira C, and Oliveira CR. ER stress is involved in Abeta-induced GSK-3beta activation and tau phosphorylation. *J Neurosci Res* 86: 2091–2099, 2008.
61. Riquelme D, Alvarez A, Leal N, Adasme T, Espinoza I, Valdés JA, Troncoso N, Hartel S, Hidalgo J, Hidalgo C, and Carrasco MA. High-frequency field stimulation of primary neurons enhances ryanodine receptor-mediated Ca^{2+} release and generates hydrogen peroxide, which jointly stimulate NF-κB activity. *Antioxid Redox Signal* 14: 1245–1259, 2011.
62. Sanz-Blasco S, Valero RA, Rodriguez-Crespo I, Villalobos C, and Nunez L. Mitochondrial Ca2+ overload underlies Abeta oligomers neurotoxicity providing an unexpected mechanism of neuroprotection by NSAIDs. *PLoS One* 3: e2718, 2008.
63. Shankar GM, Li S, Mehta TH, Garcia-Munoz A, Shepardson NE, Smith I, Brett FM, Farrell MA, Rowan MJ, Lemere CA, Regan CM, Walsh DM, Sabatini BL, and Selkoe DJ. Amyloid-beta protein dimers isolated directly from Alzheimer's brains impair synaptic plasticity and memory. *Nat Med* 14: 837–842, 2008.
64. Sharp AH, McPherson PS, Dawson TM, Aoki C, Campbell KP, and Snyder SH. Differential immunohistochemical localization of inositol 1,4,5-trisphosphate- and ryanodine-sensitive Ca2+ release channels in rat brain. *J Neurosci* 13: 3051–3063, 1993.
65. Stutzmann GE, Smith I, Caccamo A, Oddo S, Laferla FM, and Parker I. Enhanced ryanodine receptor recruitment contributes to Ca2+ disruptions in young, adult, and aged Alzheimer's disease mice. *J Neurosci* 26: 5180–5189, 2006.
66. Supnet C, Grant J, Kong H, Westaway D, and Mayne M. Amyloid-beta-(1–42) increases ryanodine receptor-3 expression and function in neurons of TgCRND8 mice. *J Biol Chem* 281: 38440–38447, 2006.
67. Tanaka J, Horiike Y, Matsuzaki M, Miyazaki T, Ellis-Davies GC, and Kasai H. Protein synthesis and neurotrophin-dependent structural plasticity of single dendritic spines. *Science* 319: 1683–1687, 2008.
68. Tong L, Balazs R, Thornton PL, and Cotman CW. Beta-amyloid peptide at sublethal concentrations downregulates brain-derived neurotrophic factor functions in cultured cortical neurons. *J Neurosci* 24: 6799–6809, 2004.
69. Tong L, Thornton PL, Balazs R, and Cotman CW. Beta - amyloid-(1–42) impairs activity-dependent cAMP-response element-binding protein signaling in neurons at concentrations in which cell survival is not compromised. *J Biol Chem* 276: 17301–17306, 2001.
70. Tu H, Nelson O, Bezprozvanny A, Wang Z, Lee SF, Hao YH, Serneels L, De Strooper B, Yu G, and Bezprozvanny I. Presenilins form ER Ca2+ leak channels, a function disrupted by familial Alzheimer's disease-linked mutations. *Cell* 126: 981–993, 2006.
71. Tyler WJ and Pozzo-Miller L. Miniature synaptic transmission and BDNF modulate dendritic spine growth and form in rat CA1 neurones. *J Physiol* 553: 497–509, 2003.
72. Vieira MN, Forny-Germano L, Saraiva LM, Sebollela A, Martinez AM, Houzel JC, De Felice FG, and Ferreira ST. Soluble oligomers from a non-disease related protein mimic Abeta-induced tau hyperphosphorylation and neurodegeneration. *J Neurochem* 103: 736–748, 2007.
73. Walsh DM, Klyubin I, Fadeeva JV, Cullen WK, Anwyl R, Wolfe MS, Rowan MJ, and Selkoe DJ. Naturally secreted oligomers of amyloid beta protein potently inhibit hippocampal long-term potentiation in vivo. *Nature* 416: 535–539, 2002.
74. Wang X, Su B, Lee HG, Li X, Perry G, Smith MA, and Zhu X. Impaired balance of mitochondrial fission and fusion in Alzheimer's disease. *J Neurosci* 29: 9090–9103, 2009.
75. Wang X, Su B, Siedlak SL, Moreira PI, Fujioka H, Wang Y, Casadesus G, and Zhu X. Amyloid-beta overproduction causes abnormal mitochondrial dynamics via differential modulation of mitochondrial fission/fusion proteins. *Proc Natl Acad Sci U S A* 105: 19318–19323, 2008.
76. Yang G, Pan F, and Gan WB. Stably maintained dendritic spines are associated with lifelong memories. *Nature* 462: 920–924, 2009.
77. Zhao W, Meiri N, Xu H, Cavallaro S, Quattrone A, Zhang L, and Alkon DL. Spatial learning induced changes in expression of the ryanodine type II receptor in the rat hippocampus. *FASEB J* 14: 290–300, 2000.
78. Zündorf G and Reiser G. Calcium dysregulation and homeostasis of neural calcium in the molecular mechanisms of neurodegenerative diseases provide multiple targets for neuroprotection. *Antioxid Redox Signal* 14: 1275–1288, 2011.

Address correspondence to:
Prof. Cecilia Hidalgo
Facultad de Medicina
Centro de Estudios Moleculares de la Célula
and Programa de Fisiología y Biofísica
Instituto de Ciencias Biomédicas
Universidad de Chile
Independencia 1027
838-0453 Santiago
Chile

E-mail: chidalgo@med.uchile.cl

Date of first submission to ARS Central, May 7, 2010; date of final revised submission, July 15, 2010; date of acceptance, August 13, 2010.

Abbreviations Used

Aβ = amyloid-β peptide
AβOs = Aβ oligomers
AD = Alzheimer's disease
BDNF = brain-derived neurotrophic factor
CCCP = carbonyl cyanide *m*-chlorophenylhydrazone
DIC = differential interference contrast
DIV = days *in vitro*
Drp-1 = dynamin-related protein 1
GFAP = glial fibrillary acidic protein
IP3 = inositol-1,4,5-trisphosphate
LTD = long-term depression
LTP = long-term potentiation
MAP2 = microtubule-associated protein
MK-801 = dizcilpine
MTT = 3-(4,5-dimethylthiazol-2-Yl)-2,5-diphenyltetrazolium bromide
NAC = *N*-acetyl-L-cysteine
NMDA = *N*-methyl-D-aspartate
NMDAR = *N*-methyl-D-Aspartate receptor
RyR = ryanodine receptor
TrKB = tropomyosin-related kinase

This article has been cited by:

1. C. D. SanMartín, A. C. Paula-Lima, C. Hidalgo, M. T. Núñez. 2012. Sub-lethal levels of amyloid #-peptide oligomers decrease non-transferrin-bound iron uptake and do not potentiate iron toxicity in primary hippocampal neurons. *BioMetals* **25**:4, 805-813. [CrossRef]
2. Michael P. Walker, Frank M. LaFerla, Salvador S. Oddo, Gregory J. Brewer. 2012. Reversible epigenetic histone modifications and Bdnf expression in neurons with aging and from a mouse model of Alzheimer's disease. *AGE* . [CrossRef]
3. C.D. SanMartin, T. Adasme, C. Hidalgo, A.C. Paula-Lima. 2012. The Antioxidant N-Acetylcysteine Prevents the Mitochondrial Fragmentation Induced by Soluble Amyloid-ß Peptide Oligomers. *Neurodegenerative Diseases* **10**:1-4, 34-37. [CrossRef]
4. Miao-Kun Sun, Daniel L. AlkonActivation of Protein Kinase C Isozymes for the Treatment of Dementias **64**, 273-302. [CrossRef]
5. M. J. Calkins, M. Manczak, P. Mao, U. Shirendeb, P. H. Reddy. 2011. Impaired mitochondrial biogenesis, defective axonal transport of mitochondria, abnormal mitochondrial dynamics and synaptic degeneration in a mouse model of Alzheimer's disease. *Human Molecular Genetics* **20**:23, 4515-4529. [CrossRef]
6. Sergio T. Ferreira, William L. Klein. 2011. The A# oligomer hypothesis for synapse failure and memory loss in Alzheimer's disease. *Neurobiology of Learning and Memory* . [CrossRef]
7. Cecilia Hidalgo , M. Angélica Carrasco . 2011. Redox Control of Brain Calcium in Health and Disease. *Antioxidants & Redox Signaling* **14**:7, 1203-1207. [Abstract] [Full Text HTML] [Full Text PDF] [Full Text PDF with Links]